Journal of
Materials Chemistry C

Accepted Manuscript

This article can be cited before page numbers have been issued, to do this please use: A. Sil, D. Giri and S. K. Patra, *J. Mater. Chem. C*, 2017, DOI: 10.1039/C7TC04178K.

ROYAL SOCIETY OF CHEMISTRY

rsc.li/materials-c

View Article Online
DOI: 10.1039/C7TC04178K

Journal Name

ARTICLE

Arylene-vinylene Terpyridine Conjugates: Highly Sensitive, Reusable and Simple Fluorescent Probes for the Detection of Nitroaromatics

Received 00th January 20xx,
Accepted 00th January 20xx

DOI: 10.1039/x0xx00000x

www.rsc.org/

Amit Sil,[a] Dipanjan Giri,[a] and Sanjib K. Patra*[a]

A series of highly emissive arylene-vinylene conjugated 4'-(4-{2-[aryl]-ethenyl}phenyl)-2,2':6',2''-terpyridines (aryl = 4-methylphenyl, 4-fluorophenyl, 1-naphthyl, and 9-anthralyl in **P1**-**P4** respectively) have been explored for the detection of nitroaromatic compounds (NACs). The synthesized push-pull fluorescent probes show remarkable sensitivity towards NACs in solution, vapor and contact mode as 'turn-off' sensor which can be visualized by naked eye. The photophysical studies reveal that the electron transfer occurs from the electron rich arylene-vinylene conjugated terpyridine to the electron deficient NACs through supramolecular complexation which is further illustrated from the time-resolved fluorescence and ^{1}H NMR titration experiment. The arylene-vinylene conjugated terpyridines offer excellent sensitivity towards picric acid (PA) exhibiting nanomolar detection in contact mode, and ppm level detection in solution state with association constants in the range of 2.54-8.08×10^{4} M^{-1}. The HOMO-LUMO energy levels have been calculated from electrochemical and TDDFT studies to understand the efficacy and the mechanism of electron transfer from probe to NACs leading to fluorescence quenching. The reversibility, recyclability and contact mode detection of PA in nanomolar level demonstrates its practical utility as solid state kit for onsite detection of NAC explosives.

Introduction

Nitro-rich compounds are essential energetic materials mostly used as component for the preparation of landmines and explosive materials.[1] For example, trinitrotoluene and picric acid are heavily used as nitroaromatic (NAC) explosives. On the other hand, nitroaromatics can deteriorate the environment through short-term or long-term exposure by contaminating the soil and water at toxic levels thus causing hazardous effects on human health such as headache, weakness, anemia, respiratory disorders, carcinogenicity, skin irritation and liver injury.[2] Large scale use of NAC explosives by terrorist groups, has prompted the scientific community to develop novel and synthetically ease sensing materials for easy, rapid, sensitive, selective and economic detection of explosives both in air and in solution.[3]

Various type of analytical methods such as energy dispersive X-ray diffraction,[4] fluorescence signaling,[3a-c,5] nuclear quadruple resonance,[6] ion mobility spectrometers,[7] surface enhanced Raman spectroscopy,[8] chromatography using an ultraviolet absorption detector,[9] mass spectrometry,[10] thermal neutron analysis,[11] and electrochemical assay,[12] are being used for NACs detection in solution and in vapor phase. Among them, fluorescence signaling is advantageous because of its high sensitivity, quick response, cost efficiency, portability, and operational simplicity. A considerable number of fluorescent probes including polymers,[3c,5a,13] gels,[14] small molecule sensors,[15] nanoparticles,[16] nano fibers[17] and MOFs[18] have been developed for the detection of NACs. Although the rigid π-conjugated polymers show good sensitivity towards NACs through optical signal amplification effect, this class of polymeric probes suffer from solubility, processability and multistep synthetic routes in many cases which are not viable. Moreover, the detection of NACs by MOFs and nanoparticles are not often preferable for practical application as they suffer from poor solubility, complex structure and solution instability. Therefore development of novel, simple and efficient sensing probes based on small molecules which can be accessed through economic and easy synthetic strategy is now current interest to the research communities. Moreover, its well defined structure, monodispersity and convenient method of purification allow a clear understanding of the structure property relationship, and permits superior performance towards detection of NACs. The high electron deficient property of the NACs facilitates efficient photo-induced electron transfer (PET) from the electron rich π-conjugated

[a] Department of Chemistry, Indian Institute of Technology Kharagpur, Kharagpur 721302 (India); *E-mail: skpatra@chem.iitkgp.ernet.in

†Electronic Supplementary Information (ESI) available: Spectroscopic characterization of the synthesized compounds, experimental details, selected photophysical data for sensing studies electrochemical and theoretical studies, additional FESEM images. See DOI: 10.1039/x0xx00000x

View Article Online
DOI: 10.1039/C7TC04178K

fluorophores. There are a considerable number of small molecule chromophores based on pyrene, coumarins, purpurin, fluorescein, triphenylamine, hetero oligophenylene, pentacenquinone, fluoranthene and iptycene which have been employed for the detection of NACs.[15]

Arylene-vinylene conjugated terpyridines represent a new category of highly luminescent π-conjugated chromophores with chelating function and relatively long lived excited states.[19] Arylene-vinylene unit is advantageous to improve the π-conjugation enabling strong intermolecular and π-π interaction with electron deficient NACs. In this work, different aryl groups have been introduced in 4'-(4-{2-[aryl]-ethenyl}phenyl)-2,2':6',2''-terpyridyl conjugates through the vinylene linkage to tune the electronic and optical properties. The extended π-conjugation in the arylene-vinylene conjugated terpyridine is beneficial to reduce the energy of LUMO and hence the band gap of the probes, enhancing detection sensitivity. In the present work, we report facile and easy synthesis of highly fluorescent arylene-vinylene terpyridine conjugates by varying the arylene group and their detection efficiency towards NACs in solution and solid state. The unique structural modification on the arylene core and extension of π-conjugation offer interesting and favorable properties for detection of NACs, thereby improving the optical signal response.

Results and discussion

Synthesis and Characterization

Arylene-vinylene unit has been chosen as a sensing probe for the detection of NACs for its enlarged π-conjugation to enhance the fluorescence response and also for its emission in the visible range. The reasons for selecting terpyridyl (*tpy*) moiety are twofold. Firstly, it can efficiently act as donor unit inducing tunable ICT band emission. Secondly, being a Lewis base, pyridyl 'N' can act as proton abstractor and as synthon for H-bonding offering beneficial supramolecular interaction between probe and analyte. Moreover, the presence of highly π-conjugated backbone with *tpy* unit favors the formation of strong intermolecular and π-π interaction with electron deficient NACs. Most importantly, the syntheses of the probes are very simple and economic. A series of arylene-vinylene conjugated terpyridines were synthesized by varying the electron donating and withdrawing nature of the arylene groups to tune their photophysical and consequently the sensing properties. The synthetic protocol for preparing 4'-(4-{2-[aryl]-ethenyl}phenyl)-2,2':6',2''-terpyridine (**P1**-**P4**) is outlined in Scheme 1 following a stepwise approach starting from 4'-(4-methylphenyl)-2,2':6',2''-terpyridine (**1**). Compound **1** was synthesized following Kröhnke method involving the condensation of 4-methylbenzaldehyde with two equivalent of acetyl pyridine followed by the formation of the central pyridine ring in ethanol using ammonia as a base.[20] NBS-mediated allylic bromination of **1** was achieved by catalytic amount of 2,2'-azobisisobutyronitrile (AIBN) to furnish **2**, which upon reacting with PPh_3 in refluxing toluene yielded the phosphonium ylide (**3**) as evidenced by $^{31}P\{^1H\}$ NMR showing a singlet at 23.7 ppm (in $CDCl_3$). Finally, a series of highly luminescent fluorophores appended with *tpy* was achieved by Wittig condensation between the aryl aldehyde and **3** in presence of *t*-BuOK in solvent free mild condition by grinding in a mortar as *green* and economic synthetic protocol reducing the use of hazardous organic solvents.[19g] The luminescent arylene-vinylene conjugated terpyridines (**P1**-**P4**) were unambiguously characterized by multinuclear NMR and HRMS (ESI, +ve) analyses. $^{19}F\{^1H\}$ NMR ($CDCl_3$) spectrum of **P2** shows one characteristic singlet at -114.1 ppm. ^1H NMR ($CDCl_3$) of compound **P1** shows one singlet at 2.37 ppm for the methyl protons. The naphthyl and anthracenyl protons in **P3** and **P4**

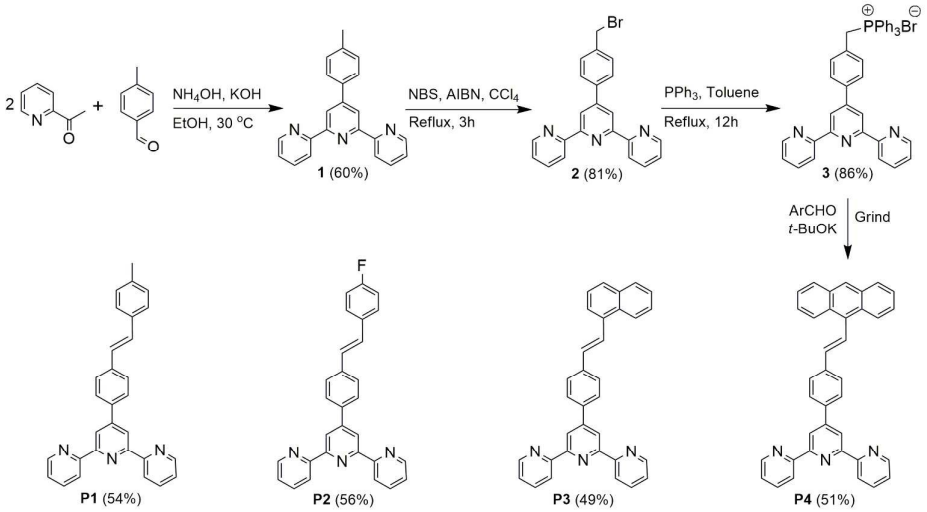

Scheme 1 Synthetic route for the probes **P1**-**P4**, (ArCHO = 4-methylbenzaldehyde, 4-fluorobenzaldehyde, 1-naphthaldehyde, and 9-anthraldehyde for **P1**-**P4** respectively). Yields are in the parenthesis.

View Article Online
DOI: 10.1039/C7TC04178K

resonate as multiplet in the region of 7.88-8.69 ppm and 7.89-8.43 ppm respectively. In $^{13}C\{^{1}H\}$ NMR spectra, the methyl carbon in probe **P1** resonates at 21.6 ppm. The carbons of the aromatic rings for all the probes appear in the region of 115.3–156.6 ppm. More importantly, the two vinylene protons resonate in the range of 6.97-7.38 ppm as doublets with $J \geq 16.0$ Hz in ^{1}H NMR spectra, confirming the *trans*-vinylene linkage (ESI†). The *trans*-vinylene linkage is necessary to acquire the extended π-delocalization as also noticed from the molecular structure of **P4** and similar terpyridyl conjugate, 4'-(4-(2-(4-(N,N-diphenylamino)phenyl)ethenyl)phenyl)-2,2':6',2''-terpyridine obtained from single crystal X-ray crystallography.[19d,g] Despite several attempts, we were not successful to grow crystals of the newly synthesized **P2** and **P3** probes, suitable for single crystal X-ray diffraction studies. The formation of the probes was further confirmed by mass spectrometric analyses (HRMS) exhibiting the molecular ion peaks ($[M+H]^+$) with the expected isotopic distribution pattern (ESI†).

Photophysical properties

The very good solubility in common organic solvents allowed us to study the photophysical properties of the π-electron rich arylene-vinylene conjugated terpyridines. The photophysical properties of the synthesized probes (**P1**-**P4**) were studied in $CHCl_3$ in 1×10^{-5} M concentration at ambient temperature. Each of the probes showed a lower energy absorption band at λ_{max} of 334-390 nm in addition to a relatively higher energy absorption in the region of 258-285 nm (λ_{max}) as shown in Fig. 1. The high energy absorption is assigned as intra-ligand charge transfer (ICT) transition while the low energy band is ascribed as π to π* transition of the conjugated molecular backbone. The low energy absorption maxima for **P1**, **P3** and **P4** is gradually red shifted with increasing number of fused aromatic rings indicating enhanced π-delocalization. The solid state absorption spectra were recorded on thin film samples made by spin-coating of the probe solution on quartz plates. The solid state absorption of the arylene-vinylene conjugated terpyridines (**P1**-**P4**) follow the similar trend but red shifted by 12–18 nm with relatively broad absorption spectra in comparison to the solution state spectra, presumably due to strong intermolecular π–π stacking interactions (Table S2, ESI†). The coexistence of multiple degree of aggregation in thin film is supported by the broad nature of the absorption spectra.[21] The energy band gap of the probes was accounted by inspecting the edge of the solid state absorption spectra, using the equation $E_g^{opt}(eV) = 1240/\lambda_{cut\ off}$. The optical band gap values of **P1**-**P4** were found to be 3.0, 3.03, 2.95 and 2.66 eV respectively.

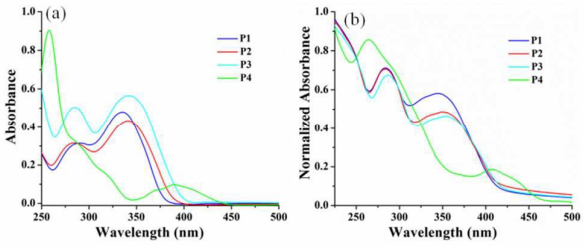

Fig. 1 Absorption spectra of **P1**-**P4** (a) in $CHCl_3$ (1×10^{-5} M) (b) on thin film (spin coated on quartz plate) at ambient temperature.

The emission spectra of **P1**-**P4** were recorded in $CHCl_3$ as 1×10^{-5} M concentration at ambient temperature (28 °C). Interestingly, the probes showed a gradual bathochromic shift in photoluminescence spectra with λ_{em} from 417 nm to 498 nm exhibiting blue to green fluorescence while going from **P1** to **P4**. In case of **P1**-**P3**, the compounds showed blue fluorescence with emission maxima at 417, 435 and 437 nm respectively whereas **P4** exhibited green fluorescence with emission maxima at 498 nm as shown in Fig. 2. The solid state emission maxima for all the arylene-vinylene conjugated terpyridines (**P1**-**P4**) showed bathochromic shift from the solution state emission maxima, and were found to be 435, 440, 458 and 504 nm respectively (Fig. S28 in ESI†).The fluorescence quantum yields (Φ) of all the sensing probes were measured in $CHCl_3$ using quinine sulfate (Φ = 0.54) in 0.1 M H_2SO_4 solution as a reference at ambient temperature (28 °C).[22] The PL quantum yields of the fluorophores are in the range of 0.23-0.36, showing a gradual enhancement with increasing π-conjugation. The photophysical data of all the arylene-vinylene conjugated terpyridines are summarized in Table 1.

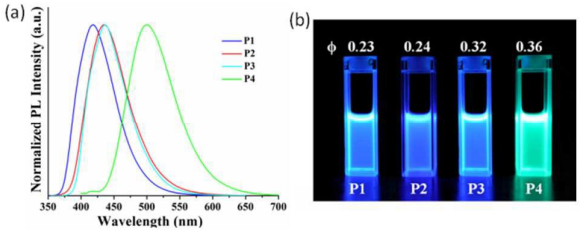

Fig. 2 (a) Emission spectra of **P1**-**P4** in $CHCl_3$ (1×10^{-5} M) at ambient temperature. (b) Visual appearance of **P1**-**P4** in $CHCl_3$ (1×10^{-5} M) under UV illumination at 365 nm.

View Article Online
DOI: 10.1039/C7TC04178K

Table 1 Photophysical data of the probes in chloroform at 28 °C.

Probes	λ_{abs}, nm (Logε)	λ_{em}, nm (λ_{ex})	Stokes Shift, cm^{-1}	Φ (%)[a]	Lifetime ns[b]
P1	334(4.68), 285(4.49)	417(334)	1666	23	1.36
P2	339(4.63), 283(4.50)	435(339)	1517	24	0.94
P3	341(4.74), 284(4.69)	437(341)	1552	32	1.91
P4	390(4.0), 258(4.95)	498(390)	1798	36	2.88

[a]Quinine sulphate (0.1 M H_2SO_4; Φ = 0.54) was used as reference for quantum yield calculation; [b]Life time was measured by TCSPC method (*vide infra*); ε = Absorption coefficient ($M^{-1}cm^{-1}$.).

It is well known in literature that the π–π interaction in planar polyaromatic compounds induces intermolecular aggregation in solution.[15e,23] The concentration dependent emission spectra of the sensing probes was carried out in $CHCl_3$ to determine the optimum concentration undergoing the minimum self-aggregation. We were unable to record the concentration-dependent UV-Vis spectroscopic analysis as the absorbance of the compounds exceeded the instrument limit at higher concentration. For example, the intensity of the emission band decreases with a red-shift in emission maxima from 498 to 512 nm (λ_{em}) for **P4** with increasing concentration from 10^{-5} to 10^{-3} M. This clearly demonstrates that the self-assembled aggregates are formed in higher concentration (~10^{-3} M) due to π-π interaction inducing fluorescence quenching. However, this band was blue shifted to 498 nm when the solution was diluted to 10^{-5} M. This behavior of the fluorescence spectra attributed the dissociation of the aggregates to form unimers in lower concentrated solution. The fluorescence intensity of the emission maxima decreased when the compound solution was diluted to 10^{-6} M. The other arylene-vinylene conjugated terpyridines also showed similar concentration-dependent fluorescence spectral change in the corresponding concentrated and dilute solutions (Fig. S29 in ESI†). To further confirm the formation of aggregates, the particle size of the probes was measured by dynamic light scattering (DLS) experiment in solution. DLS studies of all the probes were carried out by varying the concentration ranging from 10^{-3} to 10^{-5} M, and different particle sizes were found as expected (Fig. 3). The average aggregate size (D_H) of all the probes in relatively higher concentrated (10^{-3} M) solution was larger (D_H = 164-342 nm) with broad distribution illustrating the presence of various size of aggregates in the medium. When diluted, the distribution was relatively narrower and the aggregate size also decreased ascribing the presence of smaller particle size (D_H = 58–141 nm) of the sensing probe in solution.[13a,15i,15u] This variation in size occurs as the extent of molecular self-assembly increases in the relatively higher concentration of the probe molecules due to the favorable π–π stacking. All the arylene-vinylene conjugated terpyridines displayed less aggregation behavior with concentration of 10^{-5} M as evidenced from DLS experiments and as well as concentration-dependent fluorescence study (Fig. S30 in ESI†). Hence, the sensing application was explored in 10^{-5} M concentration to minimize the self-association behavior of the probes.

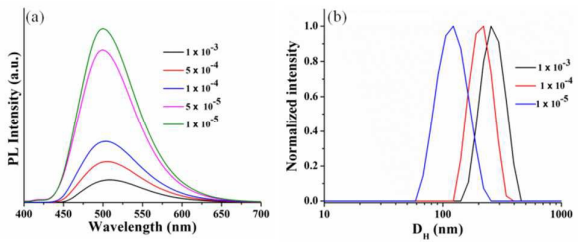

Fig. 3 Concentration dependent (a) fluorescence and (b) DLS spectra of **P4** in $CHCl_3$ solution at ambient temperature.

The highly emissive and π-electron rich nature of the arylene-vinylene conjugated terpyridines allowed us to explore their potential application as a fluorescence chemosensor. NACs are highly electron deficient molecules and can undergo strong interaction with electron rich π-conjugated fluorescent probes mainly through π-π interaction resulting change in emission properties. Keeping this in mind, all the arylene-vinylene conjugated terpyridines were employed for the detection of different NACs in $CHCl_3$. To explore the potential application, all the probes were treated with different nitroaromatic compounds such as nitrobenzene (NB), nitrotoluene (NT), 4-hydroxy nitrobenzene (HNB), 4-nitrobenzoic acid (NBA), 2,6-dinitrotoluene (DNT), and picric acid (PA). Due to the electron deficient nature of the NACs, the fluorescence intensity of the probes readily quenched upon addition of NACs as a result of facile electron transfer between the fluorophore and the NACs. Interestingly, after the addition of various nitroaromatics (with concentration of ~$1x10^{-5}$ M to ~$1×10^{-3}$ M) to the solution of **P1–P4** probes (~$1×10^{-5}$ M), different percentage of emission quenching was observed. Increase in the number of nitro groups enhances the electron deficiency in nitroaromatic molecules, and thus the extent of fluorescence quenching is increased. Therefore, on addition of picric acid the magnitude of quenching was higher than the other nitroaromatics used in this study, indicating the efficient detection sensitivity of the probes towards explosive picric acid. To prove the selectivity only towards NACs, fluorescence spectra of the sensing probes were also measured in the presence of other aromatic compounds such as chlorinated (such as 1,2-dichlorobenzene and 1,4-dichlorobenzene) and alkyl aromatics (such as toluene and mesitylene), showing no significant change in fluorescence quenching (Fig. 4).

Since the anthracene functionalized arylene-vinylene conjugated terpyridine **(P4)** exhibits highest quantum yield among the four probes in its solution state, the sensing efficacy of **P4** is discussed in detail here. To gain an insight into the sensing mechanism in more depth and to ensure the

View Article Online
DOI: 10.1039/C7TC04178K

phenomenon, fluorescence spectroscopic titrations were performed with a continuous variation of concentrations of NACs. Upon incremental addition of NACs the emission intensity of **P4** steadily quenched and no residual emission band was observed. The addition of 25 equivalents of PA to the solution of **P4** resulted almost complete quenching of fluorescence emission. The similar quenching behaviors of the other probes (**P1**-**P3**) in the presence of PA are provided in ESI (Fig. S31, ESI†). The relative emission quenching of the probes (**P1**-**P4**) towards different NACs is depicted in Fig. 4, demonstrating maximum emission quenching for PA.

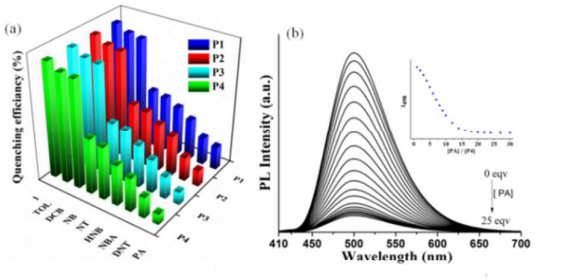

Fig. 4 (a) Quenching efficiency of all the probes (**P1**-**P4**) towards different NACs in $CHCl_3$. Probe (1), Toluene (TOL), Dichlorobenzene (DCB), Nitrobenzene (NB), Nitrotoluene (NT), *p*-Hydroxy nitrobenzene (HNB), Nitrobenzoic acid (NBA), 2.6-Dinitrobenzene (DNT), Picric acid (PA); (b) Fluorescence titration of **P4** upon incremental addition of PA; (inset) Fluorescence quenching behavior of **P4** at 498 nm.

The excellent 'turn-off' sensing behavior of **P4** towards PA encouraged us to investigate the visual change of **P4** probe in solution before and after addition of PA. Upon addition of PA, the colour of **P4** solution turned immediately from light green to intense yellow probably due to the formation of charge transfer complex with PA. More interestingly, the bright green fluorescent solution of **P4** turned to nonemissive when the solution was illuminated under 365 nm light (Fig. 5). Like **P4**, the other blue emissive probes (**P1**-**P3**) also turned to nonfluorescent immediately after treating with PA, demonstrating easy and efficient detection of PA in naked eye (Fig. S42 in ESI†)

The possibility of forming protonated species originated by

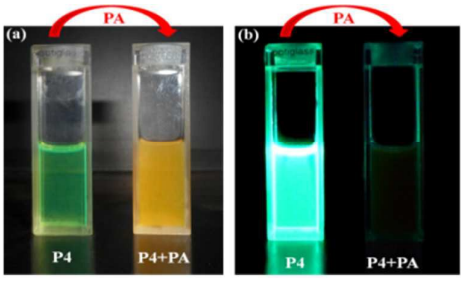

Fig. 5 Visual appearance of **P4** before and after addition of PA under (a) ambient light and (b) UV illumination at 365 nm.

excited state proton transfer from PA to the pyridyl nitrogen of the probes was ruled out as no new band formation was observed in fluorescence spectra upon treating with excess equivalent of PA to the probe. To confirm the possibility of excited state proton transfer to arylene-vinylene conjugated terpyridines, 2 µL of strong non-aromatic acid (trifluoroacetic acid) was added to **P4** solution under the same set of condition as used for PA and the corresponding fluorescence data was recorded. Interestingly, the emission band at 498 nm was disappeared with concomitant appearance of a new band centered at 588 nm with low emission intensity ascribing the slow proton transfer. The strong acidic nature of the trifluoroacetic acid induces the proton transfer which is not observed for aromatic picric acid. Under the same set of conditions, identical results were observed for the other arylene-vinylene conjugated terpyridyl probes upon addition of PA and TFA (Fig. S32 in ESI†).

To gain insight of quenching rate, the emission response of the sensing probes (**P1**-**P4**) was investigated using Stern-Volmer relationship.[15l,m] The Stern–Volmer (SV) equation is expressed as $I_o/I = 1 + K_{SV}[Q]$, where I_o and I are the fluorescence intensities in the absence and presence of the analyte (NACs), [Q] is the analyte concentration and K_{SV} is the Stern–Volmer rate constant. The SV plots reveal high binding constants of probe-NAC adducts with the highest value of K_{SV} in the order of 10^4 M^{-1}. The Stern-Volmer constants of the arylene-vinylene conjugated terpyridines towards different NACs are summarized in Table 2 (Fig. S34 in ESI†). The linear quenching response from Stern-Volmer plot upon incremental addition of NACs demonstrates the static quenching through the excited state interaction as presented in Fig. 7. These results suggest that the quenching phenomena of the fluorescent aggregates can be explained by the electron transfer and/or energy transfer process between the π-electron rich sensing probe and the electron deficient NACs.[15h-l,24] Moreover, the spectral overlap of the absorption and emission bands of the sensing probes allows the energy transfer from the excited state of the arylene-vinylene conjugated terpyridines (**P1**–**P4**) to the ground state of PA, further increasing the fluorescence quenching efficiency (Fig. S33 in ESI†).[15f] The lowest detectable concentration of PA was estimated using the linear response of fluorescence intensity of the probe with the concentration of PA to assess the sensitivity of the probes. The limit of detection (LOD)[15k] of the probes towards PA was found to be in the range of 1.31-

Table 2. Association constant (M^{-1}) of the sensing probes towards different NACs.

NACs	P1	P2	P3	P4
NB	6.64×10^3	6.67×10^3	6.69×10^3	8.08×10^3
NT	1.13×10^4	1.19×10^4	1.18×10^4	1.16×10^4
NBA	1.47×10^4	1.46×10^4	1.47×10^4	1.70×10^4
HNB	1.8×10^4	1.82×10^4	1.84×10^4	1.87×10^4
DNT	2.23×10^4	2.20×10^4	2.26×10^4	2.29×10^4
PA	2.54×10^4	2.63×10^4	2.69×10^4	8.08×10^4

View Article Online
DOI: 10.1039/C7TC04178K

2.94×10^{-7} M (31-70 ppm) signifying its applicability even in the sub-micromolar range (Fig. S35 in ESI†).

The time resolved fluorescence spectra of **P1**-**P4** in chloroform were also recorded to understand the nature of the excited states as depicted in Fig. 6. The fluorescence lifetime of all the probes were found to be in the range of 0.94-2.88 ns as measured by the time correlated single photon counting (TCSPC) method (Table 1). The fluorescence lifetime values of **P1**, **P3** and **P4** probes increase with the extended π-conjugation. However, the fluorescence lifetime of **P2** is relatively less than that of the other probes presumably due to the higher band-gap (E_g^{opt} = 3.03 eV). The fluorescence lifetime of the probes were also evaluated in the presence and absence of PA to understand the fluorescence quenching mechanism. For all the probes, the fluorescence life time values were found to be nearly invariant upon addition of incremental equivalents of PA suggesting of static quenching occurring through electron transfer from the excited state of the probe to electron deficient PA (Fig. S36 in ESI†).[15l,m,25]

To inspect the 'turn-off' sensing mechanism, HOMO and LUMO energy levels have been calculated from cyclic voltammetry experiments conducted in CH_3CN solution using n-Bu_4NPF_6 (0.1 M) as supporting electrolytes, Pt disc working electrode, Pt wire counter electrode and Ag/AgCl reference electrode (Fig. S46 in ESI†). The E_{HOMO} energy levels of **P1**-**P4**

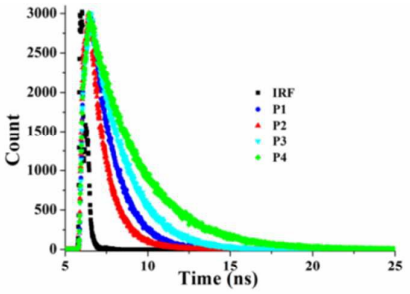

Fig. 6 Time resolved fluorescence spectra of the probes (**P1**-**P4**) in $CHCl_3$.

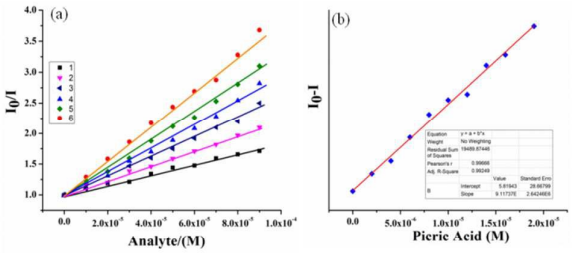

Fig. 7 (a) The Stern-Volmer plot for the **P4** towards different nitroaromatics; 1: NB, 2: NT, 3: HNB, 4: NBA, 5: DNT, 6: PA. (b) Plot for evaluation of LOD for P**4** towards PA.

were estimated as -6.02, -6.07, -6.0 and -5.91 eV respectively, based on their onset oxidation potential by considering E_{HOMO} (eV) = -(E_{ox}^{onset} + 4.71).[26] As there was no prominent reduction process for the probe molecules, the E_{LUMO} energy levels were estimated from the E_{HOMO} energy levels and its optical band gap (*vide supra*) following the equation, E_{LUMO} (eV) = E_{HOMO} + E_g^{opt}.[27] Thus, the E_{LUMO} energy levels were calculated as -3.02, -3.04, -3.05 and -3.25 eV for **P1**–**P4** respectively**.** As expected, introduction of more numbers of fused aromatic rings in the molecular backbone induces enhancement in π-conjugation resulting decrease in the HOMO-LUMO energy gap (Table 3). The LUMO energy levels of electron deficient nitroaromatics are higher than the HOMOs of the probe molecules but lower than the LUMO levels of the probes. The facile photo-induced electron transfer (PET) occurs from the LUMO of the excited probes to LUMO of the NACs followed by reverse electron transfer to the HOMO of the sensing probes in a non-radiative process resulting in fluorescence quenching as depicted in Fig. 8.[5f,15f,28]. Consequently, higher degree of fluorescence quenching was observed for the utmost electron deficient nitroaromatics such as PA due to its relatively lower LUMO energy levels. Furthermore, the presence of large π-conjugated backbone facilitates the formation of non-emissive charge transfer complex through π-π stacking interaction between the planar arylene-vinylene moiety and the nitroaromatic ring favoring electron transfer. In order to gain an insight of the structural properties and calculated HOMO/LUMO energy levels of the probes, frontier orbitals, geometry optimization for all the arylene-vinyline conjugated terpyridines was carried out using the Gaussian 03 program with B3LYP/6-31g* basis sets (Fig. S48 in ESI†).[29] The time-dependent density functional theoretical (TDDFT) studies were also performed to predict the excited state HOMO/LUMO energy levels in chloroform at the same theory level. The calculated electronic transition are summarized in Table S8 (ESI†). For **P1**-**P4**, the HOMO orbitals are delocalized on the arylene-vinylene moiety whereas LUMO orbitals are largely delocalized in the arylene-vinylene substituted phenyl conjugates and the central pyridine ring. Detection limits are based on the efficiency of the electron transfer process, which can be improved by increasing analyte–fluorophore binding interactions and matching the frontier molecular orbital energies of the fluorophore with the LUMO of the NACs. From the energy level diagram, we could observe that the optical band gaps are in the range 2.66–3.03 eV showing slight variation by changing arylene substituents on *para*-position of the phenyl group in 4'-phenyl-2,2':6',2''-terpyridine core.

To further investigate the mode of supramolecular interaction between the π-conjugated arylene-vinylene conjugated terpyridines and NACs, ^{1}H NMR spectroscopic titration studies were carried out with incremental addition of picric acid (PA) as presented in Fig. 9. The $H_{a,a'}$ and $H_{b,b'}$ pyridyl protons resonated at 8.76 and 7.81 ppm in free **P3** experienced downfield shift by 0.02 and 0.01 ppm respectively in **P3**-**PA** supramolecular complex. This downfield behavior is presumably due to the withdrawl of electron density from **P3** by PA indicating the possibility of weak H-bonding interaction. More importantly, the signal centered at 7.97 ppm for the naphthyl protons ($H_{j,k,l}$) up fielded to 7.95 ppm upon addition of PA suggesting π-π intermolecular interactions between the naphthyl moiety and the aromatic ring of PA.[15e,k] For **P4**, the similar observation was witnessed. However, signals

View Article Online
DOI: 10.1039/C7TC04178K

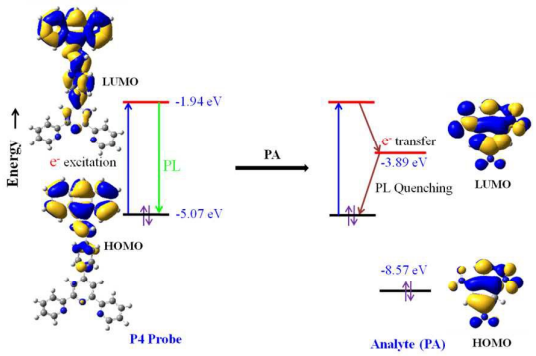

Fig. 8 Proposed electron transfer mechanism leading to PL quenching; HOMO and LUMO energy levels for **P4** and PA were calculated from theoretical calculation (Electron density distribution profiles of LUMO and HOMO of **P4** and PA were optimized with the B3LYP/6-31g* basis set).

Table 3. Evaluation of HOMO-LUMO energy levels.

Probe	HOMO (eV)[a]	LUMO (eV)[b]	E_g^{opt} (eV)
P1	-6.02(-5.45)	-3.02(-1.70)	3.0
P2	-6.07(-5.59)	-3.04 (-1.78)	3.03
P3	-6.00(-5.43)	-3.05(-1.79)	2.95
P4	-5.91(-5.07)	-3.25(-1.94)	2.66

[a] $E_{HOMO} = -(E_{ox}^{onset} + 4.71)$ eV; [b] $E_{LUMO} = (E_{HOMO} + E_g^{opt})$ eV. HOMO and LUMO energy levels from TD-DFT calculation in parenthesis.

corresponding to the anthracenyl protons were relatively complex due to the overlapping of the aromatic proton resonances. Interestingly, for **P1** and **P2** probes, the 4'-phynelene ring was involved in π-π stacking interaction with PA ring as manifested by the up field chemical shift of 4'-phynelene protons (ESI†).

The excellent 'turn-off' sensing behavior of the probes towards NACs motivated us to explore the practical application as on-site detection of picric acid. In order to demonstrate the potential utility of the sensing probes towards PA, solid state emission study was investigated by making thin film of all the arylene-vinylene conjugated terpyridine probes. The thin films were fabricated by spin coating probe solution (2 mg probe in 0.2 mL chloroform) on a quartz plate with a rate of 1000 rpm. The film was kept in a glass jar containing pinch of PA crystals at ambient temperature to measure the fluorescence response of the thin film towards PA vapour. The initial fluorescence intensity of all the probes was found to decrease gradually as a function of increasing exposure time. It was observed that the initial emission of **P4** was reduced to 37% after 60 s of exposure time, and ultimately reached to its equilibrium at 540 s by reducing the emission intensity to 81% as shown in Fig. 10. To check the reusability of the films, it was exposed to the vapor of picric acid for 420 s, and the emission spectrum was recorded. After that, the film was washed several times with milli-Q water and dried in hot air. The emission spectra of the

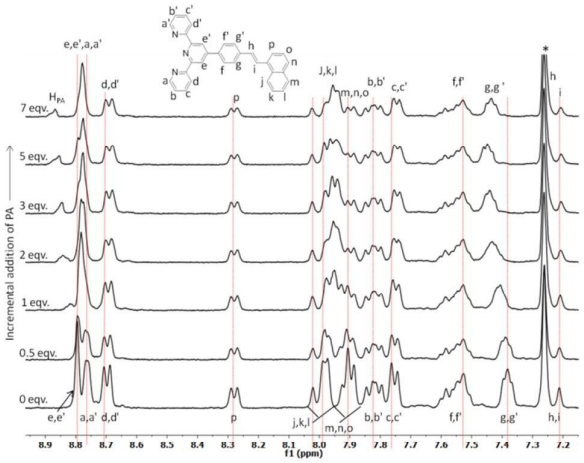

Fig. 9 Change in chemical shift of the protons in **P3** probe during ^{1}H NMR titration in $CDCl_3$ on incremental addition of PA (* = residual $CHCl_3$).

washed and dried films were recorded, and the whole process was repeated multiple times. The initial fluorescence intensity was significantly retained after repeated use of the sensing kit, indicating high reproducibility and photostability of the probe. The quenching efficiency of 42% was observed even after five cycles of exposure to picric acid (Fig. 10). Moreover, identical results were observed for the other arylene-vinylene conjugated terpyridines and the quenching behavior has been depicted in Fig. S39 (ESI†).

Nitroaromatics are also recognized as environmental contaminants polluting soil and drinking water due to short-term or long-term exposure in environment. Considering the fact, the sensing ability of the thin film was measured towards picric acid solution in submicromolar concentration. The thin film was immersed separately into the different concentration of aqueous picric acid solutions, and the percentage of fluorescence quenching was monitored by measuring the solid state emission. The study revealed that the fluorescence emission intensity was quenched by 75% for **P4** when the concentration of the picric acid was 100 μM (Fig. 11), which was clearly visible in naked eye.

The scanning electron microscopic image analyses of all the probe samples (prepared by drop casting of 5 x 10^{-4} M chloroform solution on aluminum plate) were conducted in presence and absence of picric acid to examine the change in surface morphology. All the sensing probes show porous surface morphology which is highly necessary to be a good nitroaromatic sensor by enhancing the probe-analyte interaction. **P1** showed two-dimensional rod-shaped morphology whereas leaf-like porous bed surface morphology was observed for **P2**. Interestingly, for **P3** and **P4,** hierarchical structures constructed by the three dimensional flower-like nano-objects with porous bed were detected. The porous morphology of the probes was altered to irregular shape upon treatment with PA as studied by FESEM analysis (Fig. 12).

View Article Online
DOI: 10.1039/C7TC04178K

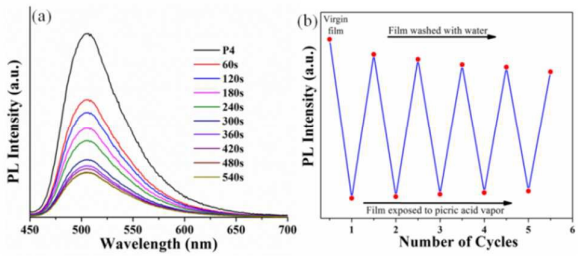

Fig. 10 (a) Quenching of fluorescence intensity of the thin film of **P4** upon exposure to PA vapor by varying exposure time; (b) Repeatability test of **P4** probe film demonstrating reusability.

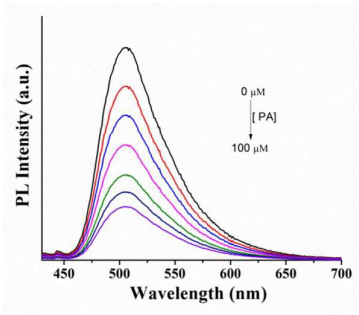

Fig. 11 Emission spectra of thin film (**P4**) after exposing aqueous PA solution by varying concentration.

Recently contact mode approach for detecting trace nitroaromatic explosives has received great attention for real time field application. Considering the porous surface nature of the probes and the efficient solution mode detection, we carried out a surface sensing approach to test the efficiency of our probes for the detection of trace nitroaromatics residue. For contact mode sensing, the filter paper (Whatman 42) test strips were dipped into the concentrated chloroform solution of the probes and dried under reduced pressure. To test the possibility, different concentration (10^{-3}-10^{-9} M) of picric acid solution in chloroform was prepared and 5 μL of each solution was spotted on each fresh test paper strips. The visual change of the fluorescence color was monitored under the illumination of 365 nm light exhibiting dark black spots for PA. The black spots were found to be prominent for the concentrated analyte solution and faded upon dilution. Remarkably, the minimum detection limit of the picric acid by the naked eye is even up to 10^{-9} M level as depicted in Fig. 13, establishing the probes (**P1**-**P4**) as excellent and efficient chemosensors for instant visual detection of trace picric acid in solution and as well as in solid state (Fig. S41 in ESI†).

Conclusions

In conclusion, we have successfully demonstrated that the highly emissive arylene-vinylene conjugated terpyridines with tunable fluorescence properties by varying the aromatic substituents on arylene-vinylene unit can act as efficient

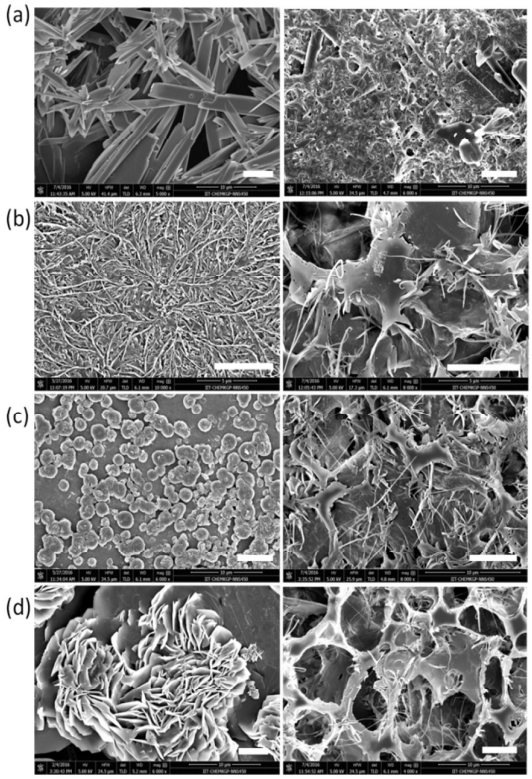

Fig. 12 FESEM images of the sensing probes before (left) and after (right) treating with PA a) **P1**, b) **P2**, c) **P3**, d) **P4** (Samples were prepared by drop casting of $5x10^{-4}$ M chloroform solution on aluminum plate); Scale bar: 5 μm.

chemosensor for the detection of nitroaromatics both in solution and solid state. The detail photophysical, electrochemical and sensing studies including life time measurement suggest that the fluorophores behave as 'turn off' sensor through static quenching induced by PET from the photo-excited probe to the electron deficient nitroaromatics, as a result of favorable HOMO-LUMO energy levels, by supramolecular complex formation as evidenced by ^{1}H NMR titration. The sensing ability of the probes **P1-P4** towards NACs as filter paper strips was successfully examined to demonstrate the practical utility as on-site detection kit for

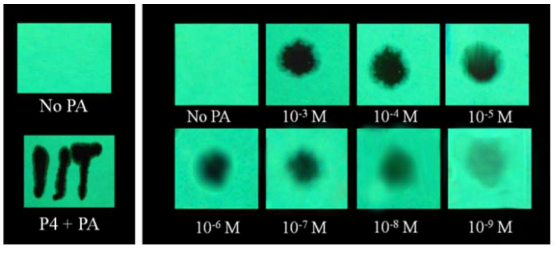

Fig. 13. Visual detection of PA of different concentration by the paper test strips coated with **P4** probe (under 365 nm light) demonstrating remarkable sensitivity towards trace PA upto nanomolar level.

View Article Online
DOI: 10.1039/C7TC04178K

nanomolar level visual detection of NACs. This work clearly reveals a novel platform for further development of simple, easily processable, selective, highly sensitive, economic and reusable chemosensor for explosive and environmentally pollutant NACs. For further improvement of sensitivity and efficacy, efforts to the structural modifications of the arylene-vinylene conjugates by fine tuning of electronic properties is underway in our laboratory. Highly blue-green light emitting nature of this unique class of functionizable arylene-vinylene terpyridinyl conjugates in solution and in solid state with good photostability can also be explored for developing as active component in organic light emitting devices.

Experimental Section

Materials and methods have been described in ESI†.

Synthesis and characterization

Compounds **1**-**3** have been synthesized following the literature procedure (ESI†).[19c]

Synthesis of 4'-(4-{2-[p-Tolyl]-ethenyl}phenyl)- 2,2':6',2''-terpyridine (P1)

4-(2,2':6',2''-Terpyridyl-4')-benzyl triphenylphosphonium bromide (1.0 g, 3.1 mmol) and potassium *tert*-butoxide (2.08 g, 18.6 mmol) were combined using a mortar and pestle, and the yellow medium was aggregated until a light orange powder formed. To it 4-methylbenzaldehyde (0.56 mL, 4.65 mmol) was added and the combined mixture was grinded vigorously for about 30 min. After the mixture became sticky, 5ml of dichloromethane was added and the mixture was continuously grinded for another 10 min. After completion of the reaction (monitored by TLC), the mixture was dispersed in 100 mL of dichloromethane and worked up with brine solution followed by water. The organic part was collected and dried over anhydrous $MgSO_4$, filtered and concentrated. The solid residue was stirred in distilled methanol for overnight at room temperature. The precipitated solid was isolated by vacuum filtration, washed with water (3×10 mL), methanol (5×10 mL) and diethyl ether (3×10 mL). The solid residue was further purified by column chromatography (ethyl acetate: hexanes, 4:1) on silica gel (60 - 120 mesh) to achieve analytically pure lemon yellow solid product. Yield: 0.71 g (54%). The characterization data were identical to those previously reported by us following a different synthetic approach (ESI†).[19h]

4'-(4-{2-[4-Fluorophenyl]-ethenyl}phenyl)-2,2':6',2'' terpyridine (P2)

P2 was prepared using a similar procedure as that for **P1** using 4-(2,2':6',2''-terpyridyl-4')-benzyl triphenylphosphonium bromide (1.0 g, 3.1 mmol) and potassium *tert*-butoxide (2.08 g, 18.6 mmol) and 4-fluorobenzaldehye(0.58 mg, 4.65 mmol). The solid residue was further purified by column chromatography (ethyl acetate: hexanes, 4:1) on silica gel (60-120 mesh) to achieve analytically pure white solid product. Yield: 0.74 g (56%); ^{1}H NMR ($CDCl_3$, 400 MHz): δ, 6.98 (d, J = 8 Hz, 2H), 7.07-7.11 (m, 2H), 7.35-7.38 (m, 4H), 7.50 (d, J = 8 Hz, 2H), 7.63 (d, J = 8 Hz, 2H), 7.89-7.94 (m, 4H, py), 8.68 (d, J = 8 Hz, 2H, py), 8.74 - 8.77 (m, 4H, py) ; ^{13}C{^{1}H} NMR ($CDCl_3$, 100 MHz): δ 115.3, 115.6, 115.8, 118.6, 121.5, 124.0, 126.3, 126.9, 127.7, 128.0, 129.1, 129.5, 129.5, 137.0, 137.3, 149.3, 156.1, 156.5. ^{19}F{^{1}H} ($CDCl_3$, 376 MHz): 114.1 ppm. HRMS (ESI^+): $C_{29}H_{21}N_3F_1$, Calculated value 430.1720 ($[M+H]^+$); experimental 430.1719 ($[M+H]^+$); FTIR (KBr, cm^{-1}): 2923 ($\bar{\upsilon}_{C\text{-}H\ stretching}$), 1586 ($\bar{\upsilon}_{C=C\ stretching}$), 1514 ($\bar{\upsilon}_{C=N\ stretching}$); λ_{max}(ε): 339 nm (4.3×10^4 $M^{-1}cm^{-1}$), 283 nm (3.2×10^4 $M^{-1}cm^{-1}$); λ_{em}: 435 nm (λ_{ex}: 339 nm).

4'-(4-{2-[2-Naphthyl]-ethenyl} phenyl)- 2,2':6',2''-terpyridine (P3)

P3 was prepared analogously to **P1** using 1-naphthaldehyde (0.60 mL, 4.65 mmol), 4-(2,2':6',2''-terpyridyl-4')-benzyl triphenylphosphonium bromide (1.0 g, 3.1 mmol) and potassium *tert*-butoxide (2.08 g, 18.6 mmol). The pure product was isolated as pale yellow solid after purification by column chromatography (ethyl acetate: hexanes, 4:1) on silica gel (60-120 mesh). Yield: 0.70 g (49%); ^{1}H NMR ($CDCl_3$, 400 MHz): δ 7.21 -7.26 (m, 2H), 7.36-7.39 (m, 2H), 7.50-7.58 (m, 2H), 7.74-7.76 (m, 2H, py), 7.80-7.84 (m, 2H, py), 7.88-7.92 (m, 3H), 7.98-8.02 (m, 3H), 8.28 (d, J = 8Hz,1H), 8.70 (d, J = 8 Hz, 2H, py), 8.75-8.76 (m, 2H, py), 8.8 (s, 2H, py); ^{13}C{^{1}H} NMR ($CDCl_3$, 100 MHz): δ 118.9, 121.7, 124.0, 125.9, 126.5, 126.9, 127.1, 127.6, 127.9, 128.5, 128.9, 129.2, 129.9, 131.3, 131.7, 134.0, 135.1, 137.2, 137.9, 138.7, 149.3, 150.0, 156.2, 156.5; HRMS (ESI^+): $C_{33}H_{24}N_3$, Calculated value 462.1970 ($[M+H]^+$); experimental 462.1967 ($[M+H]^+$); FTIR (KBr, cm^{-1}): 2926 ($\bar{\upsilon}_{C\text{-}H\ stretching}$), 1577 ($\bar{\upsilon}_{C=C\ stretching}$), 1566 ($\bar{\upsilon}_{C=N\ stretching}$); λ_{max}(ε): 344 nm (2.7×10^4 $M^{-1}cm^{-1}$), 284 nm (3.3×10^4 $M^{-1}cm^{-1}$); λ_{em}: 433 nm (λ_{ex}: 344 nm).

4'-(4-{2-[9-Anthryl]-ethenyl}phenyl)- 2,2':6',2''-terpyridine (P4)

P4 was prepared using a similar procedure as that for **P1** using 9-anthraldehyde (0.9 g, 4.65 mmol), 4-(2,2':6',2''-Terpyridyl-4')-benzyl triphenylphosphonium bromide (1.0 g, 3.1 mmol) and potassium *tert*-butoxide (2.08 g, 18.6 mmol). The pure product was isolated as bright yellow solid after purification by column chromatography (ethyl acetate: hexanes, 4:1) on silica gel (60-120 mesh). Yield: 0.32 g, (51%); ^{1}H NMR ($CDCl_3$, 400 MHz): δ 7.04 (d, J = 16.8 Hz, 1H), 7.37-7.40 (m, 2H), 7.47-7.51 (m, 4H), 7.82 (d, J = 8.4 Hz, 2H), 7.89-7.93 (m, 4H), 8.02-8.06 (m, 4H), 8.39-8.43 (m, 3H), 8.68-8.77 (m, 4H, py), 8.83 (s, 2H, py); ^{13}C{^{1}H} NMR ($CDCl_3$, 100 MHz): δ 118.9, 121.6, 124.0, 124.3, 125.5,126.4, 126.9, 127.4, 127.7, 127.9, 128.4, 128.9, 129.3, 129.9, 131.8, 132.7, 137.1, 138.1, 149.4, 149.9, 156.2, 156.5; LCMS (ESI^+): $C_{37}H_{28}N_3$, Calculated value 512.2 ($[M+H]^+$); experimental 512.4 ($[M+H]^+$); FTIR (KBr, cm^{-1}): 2924 ($\bar{\upsilon}_{C\text{-}H\ stretching}$), 1584 ($\bar{\upsilon}_{C=C\ stretching}$), 1569 ($\bar{\upsilon}_{C=N\ stretching}$); λ_{max}(ε): 391 nm

View Article Online
DOI: 10.1039/C7TC04178K

(1.5×10^4 $M^{-1}cm^{-1}$), 286 nm (3.1×10^4 $M^{-1}cm^{-1}$); λ_{em}: 498 nm (λ_{ex}: 391 nm).

Acknowledgements

Authors acknowledge the support from the DST-SERB, India through Fast Track scheme (SB/FT/CS-010/2012). SKP thanks IIT Kharagpur for funding the purchase of the electrochemical workstation through Competitive Research Infrastructure Seed Grant (SGIRG, IIT/SRIC/CHY/PBR/2014-15/44). AS and DG acknowledge IIT KGP for doctoral fellowship.

References

1 (a) J. Akhavan, *The Chemistry of Explosives*, RSC, 2004, Cornwall, UK; (b) G. I. Sunahara, G. Lotufo, R. G. Kuperman and J. Hawari, *Ecotoxicology of explosives.* Boca Raton, London, New York: CRC Press Taylor & Francis, 2009; (c) A. W. Czarnik, *Nature*, 1998, **394**, 417.

2 (a) J. Shen, J. Zhang, Y. Zuo, L. Wang, X. Sun, J. Li, W. Han and R. He, *J. Hazard. Mater.,* 2009, **163**, 1199; (b) J. D. Rodgers and N. J. Bunce, *Water Res*., 2001, **35**, 2101; (c) R. Garg, D. Grasso and G. Hoag, *Hazard. Waste Hazard. Mater*., 1991, **8**, 319; (d) S. Letzel, T. Göen, M. Bader, J. Angerer and T. Kraus, *Occup Environ Med*., 2003, **60**, 483.

3 (a) Y. Salinas, R. M. Manez, M. D. Marcos, F. Sancenon, A. M. Costero, M. Parra and S. Gil, *Chem. Soc. Rev.,* 2012, **41**, 1261; (b) M. E. Germain and M. J. Knapp, *Chem. Soc. Rev.,* 2009, **38**, 2543; (c) S. J. Toal and W. C. Trogler, *J. Mater. Chem*., 2006, **16**, 2871; (d) R. L. Woodfin, *Trace Chemical Sensing of Explosives*, John Wiley & Sons Inc. Hoboken, NJ, 2007; (e) T. F. Jenkins, D. C. Leggett and T. A. Ranney, *US Army Cold Regions Research and Engineering Laboratory*, Special Report 99, Hanover, 1999; (f) M. Krausa and A. A. Reznev, *Vapor and trace detection of explosives for antiterrorism purposes*. Boston: Kluwer Academic Publisher, 2004; (g) K. L. Diehl and E. V. Anslyn, *Chem Soc Rev*., 2013, **42**, 8596.

4 (a) R. D. Luggar, M. J. Farquharson, J. A. Horrocks and R. J. Lacey, *X-Ray Spectrom*., 1998, **27**, 87; (b) K. Wells and D. A. Bradley, *Appl. Radiat. Isot.,* 2012, **70**, 1729.

5 (a) W. Samuel, I. Thomas, G. D. Joly and T. M. Swager, *Chem. Rev.,* 2007, **107**, 1339; (b) Y. Long, H. Chen, Y. Yang, H. Wang, Y. Yang, N. Li, K. Li, J. Pei and F. Liu, *Macromolecules,* 2009, **42**, 6501; (c) A. Rose, Z. Zhu, C. F. Madigan, T. M. Swager and V. Bulovic, *Nature* 2005, **434**, 876; (d) M. S. Meaney and V. McGuffin, *Anal. Bioanal. Chem.,* 2008, **391**, 2557; (e) D.T. McQuade, A.E. Pullen and T. M. Swager, *Chem. Rev*., 2000, **100**, 2537; (f) X. Sun, Y. Wang and Y. Lei, *Chem. Soc. Rev*., 2015, **44**, 8019.

6 V. P. Anferov, G. V. Mozjoukhine and R. Fisher, *Rev. Sci. Instrum.,* 2000, **71***,* 1656.

7 (a) E. Wallis, T. M. Griffin, N. Popkie, Jr., M. A. Eagan, R. F. McAtee, D. Vrazel and J. McKinly, *Proc. SPIE–Int. Soc. Opt. Eng*., 2005, **5795**, 54; (b) G. A. Eiceman and J. A. Stone, *Anal. Chem*., 2004, **76**, 390; (c) K. M. Roscioli, E. Davis, W. F. Siems, A. Mariano, W. Su, S. K. Guharay and H. H. Hill, Jr, *Anal. Chem.,* 2011, **83***,* 5965.

8 (a) J. M. Sylvia, J. A. Janni, J. D. Klein and K. M. Spencer, *Anal. Chem*., 2000, **72**, 5834; (b) P. D. Enlow, M. Buncick, R. J. Warmack and T. V. Dinh, *Anal. Chem.,* 1986, **58**, 1119; (c) K. Vijayarangamuthu and S. Rath, *Int. J. Appl. Ceram. Technol.,* 2015,**12**, 790.

9 (a) R. Hodyss and J. L. Beauchamp, *Anal. Chem*., 2005, **77**, 3607; (b) R. V. Taudte, A. Beavis, L. W. Wilde, C. Roux, P. Doblea and L. Blanes, *Lab Chip*, 2013, **13**, 4164.

10 (a) A. Popov, H. Chen, O. N. Kharybin, E. N. Nikolaev and R. G. Cooks, *Chem. Commun*., 2005, 1953.

11 C. Vourvopoulos and P. C. Womble, *Talanta,* 2001, **54**, 459.

12 (a) M. Krausa, K. Schorb, *J. Electroanal. Chem*. 1999, *461*, 10; (b) X. Fua, R. F. Bensona, J. Wang and D. Fries, *Sens. Actuators B,* 2005, **106**, 296; (c) J. C. Chen, J. L. Shih, C. H. Liu, M. Y. Kuo and J. M. Zen, *Anal. Chem.,* 2006, **78***,* 3752.

13 (a) S. Shanmugaraju, C. Dabadie, K. Byrne, A. J. Savyasachi, D. Umadevi, W. Schmitt, J. A. Kitchenc and T. Gunnlaugsson, *Chem. Sci.,* 2017, **8**, 1535; (b) L. L. Zhou, M. Li, H. Y. Lu and C. F. Chen, *Polym. Chem*., 2016, **7**, 310; (c) W. Dong, J. Pina, Y. Pan, E. Preis, J. S. S. D. Melo and U. Scherf, *Polymer,* 2015, **76**, 173; (d) J. L. Novotney and W. R. Dichtel*, ACS Macro Lett*., 2013, **2**, 423; (e) H. Nie, G. Sun, M. Zhang, M. Baumgarten and K. M_llen, *J. Mater. Chem.,* 2012, **22**, 2129; (f) H. Nie, Y. Zhao, M. Zhang, Y. Ma, M. Baumgarten and K. Mullen, *Chem. Commun*., 2011, **47***,* 1234; (g) M. E. Germain and M. J. Knapp, *Chem. Soc. Rev.,* 2009, **38**, 2543; (h) J. S. Yang and T. M. Swager, *J. Am. Chem. Soc.,* 1998, **120**, 11864; (i) J. S. Yang and T. M. Swager, *J. Am. Chem. Soc.,* 1998, **120**, 5321; (j) G. Nagarjuna, A. Kumar, A. Kokil, K. G.Jadhav, S. Yurt, J. Kumar and D. Venkataraman, *J. Mater. Chem.,* 2011, **21**, 16597.

14 (a) V. Bhalla, A. Gupta, M. Kumar, D. S. S. Rao and S. K. Prasad, *ACS. Appl. Mater. Interfaces,* 2013, **5**, 672; (b) N. Dey, S. K. Samanta and S. B. Bhattacharya, *ACS. Appl. Mater., Interfaces,* 2013, **5**, 8394; (c) K. K. Kartha, S. S. Babu, S. Srinivasan and A. Ajayaghosh, *J. Am. Chem. Soc.* 2012, **134**, 4834; (d) K. Liu, T. Liu, X. Chen, X. Sun and Y. Fang, *ACS. Appl. Mater. Interfaces,* 2013, **5**, 9830; (e) S. Barman, J. A. Garg, O. Blacque, K. Venkatesan and H. Berke, *Chem. Commun*., 2012, *48*, 11127; (f) C. Yao, Q. Lu, X. Wang and F. Wang, *J. Phys. Chem. B,* 2014, **118**, 4661.

15 (a) R. Sodkhomkhum, M. Masik, S. Watchasit, C. Suksai, J. Boonmak, S. Youngme, N. Wanichacheva and V. Ervithayasuporn, *Sens and Actuators B,* 2017, **245**, 665; (b) E. V. Verbitskiy, A. A. Baranova, K. I. Lugovik, K. O. Khokhlov, E. M. Cheprakova, M. Z. Shafikov, G. L. Rusinov, O. N. Chupakhin and V. N. Charushin, *Dyes and Pigments,* 2017, **137**, 360; (c) S. Kaur, V. Bhalla, V. Vij and M. Kumar, *J. Mater. Chem. C,* 2014, **2**, 3936; (d) A. Chowdhury, P. Howlader and P. S. Mukherjee, *Chem. Eur. J.,* 2016, **22**, 7468; (e) B. Roy, A. K. Bar, B. Gole and P. S. Mukherjee, *J. Org. Chem*., 2013, **78**, 1306; (f) S. Kaur, A. Gupta, V. Bhalla and M. Kumar, *J. Mater. Chem. C*, 2014, **2**, 7356; (g) J. D. Xiao, L. G. Qiu, F. Ke, Y. P. Yuan, G. S. Xu, Y. M. Wanga and X. Jiang, *J. Mater. Chem. A,* 2013, **1**, 8745; (h) Y. Chandrasekaran, N. Venkatramaiah and S. Patil, *Chem. Eur. J*., 2016, **22**, 5288; (i) A. Chowdhury and P. S. Mukherjee, *J. Org. Chem.,* 2015, **80***,* 4064; (j) S. Shanmugaraju and P. S. Mukherjee, *Chem. Commun.,* 2015, **51**, 16014 and references there in; (k) N. Venkatramaiah, A. D. G. Firmino, F. A. Almeida Paz and J. P. C. Tome, *Chem. Commun.,* 2014, **50**, 9683; (l) S. Kumar, N. Venkatramaiah and S. Patil, *J. Phys. Chem. C,* 2013, **117**, 7236; (m) N. Venkatramaiah, S. Kumar and S. Patil, *Chem. Commun*., 2012, **48**, 5007; (n) V. Vajpayee, H. Kim, A. Mishra, P. S. Mukherjee, P. J. Stang, M. Lee, H. K. Kim and K. W. Chi, *Dalton Trans.,* 2011, **40**, 3112; (o) S. Shanmugaraju, S. A. Joshi and P. S. Mukherjee, *Inorg. Chem.,* 2011, **50**, 11736; (p) T. Liu, L. Ding, G. He, Y. Yang, W. Wang and Y. Fang, *ACS Appl. Mater. Interfaces,* 2011, **3**, 1245; (q) M. E. Germain and M. J. Knapp, *J. Am. Chem. Soc*., 2008, **130**, 5422; (r) G. He, H. Peng, T. Liu, M. Yang, Y. Zhang and Y. Fang, *J. Mater. Chem*., 2009, **19**, 7347; (s) P.

View Article Online
DOI: 10.1039/C7TC04178K

Anzenbacher Jr., L. Mosca, M. A. Palacios, G. V. Zyryanov and P. Koutnik, *Chem. Eur. J.,* 2012, **18**, 12712; (t) J. Yu, Y. Chen, J. J. Lia and Y. Liu, *J. Mater. Chem. C*, 2017, **5**, 799; (u) A. Chowdhury, P. Howlader and P. S. Mukherjee, *Chem. Eur. J.* **2016**, *22*, 1424.

16 (a) B. B. Chen, Z. X. Liu, H. Y. Zou and C. Z. Huang, *Analyst,* 2016, **141**, 2676; (b) Z. Yang and X. Dou, *Adv. Funct. Mater.,* 2016, **26**, 2406; (c) F. Akhgari, H. Fattahi and Y. M. Oskoei, *Sens and Actuators B,* 2015, **221**, 867; (d) Y. Ma, H. Li, S. Peng and L. Wang, *Anal. Chem*., 2012, **84**, 8415; (e) L. Feng, H. Li, Y. Qu and C. Lu, *Chem. Commun*., 2012, **48**, 4633; (f) S. S. R. Dasary, A. K. Singh, D. Senapati, H. Yu and P. C. Ray, *J. Am. Chem. Soc.,* 2009, **131**, 13806; (g) Y. Jiang, H. Zhao, N. Zhu, Y. Lin, P. Yu and L. Mao, *Angew. Chem. Int. Ed*., 2008, **47**, 8601.

17 (a) Y. Yag, H. Wang, K. Su, Y. Long, Z. Peng, N. Li and L. Feng, *J. Mater. Chem.,* 2011, **21**, 11895; (b) Y. Z. Liao, V. Strong, Y. Wang, X. Li, X. Wang and R. B. Kaner, *Adv. Funct. Mater.,* 2012, **22**, 726.

18 (a) C. L. Liu, L. P. Zhou, D. Tripathy and Q. F. Sun, *Chem. Commun.,* 2017, **53**, 2459; (b) Y. Zhang, B. Li, H. Ma, L. Zhanga and W. Zhang, *J. Mater. Chem. C*, 2017, **5**, 4661; (c) F. Wang, Z. Yu, C. Wang, K. Xu, J. Yu and J. Zhang, *Sens. and Actuators B,* 2017, **239**, 688; (d) M. Bagheri, M.Y. Masoomi, A. Morsali and A. Schoedel, *ACS Appl. Mater. Interfaces,* 2016, **8***,* 21472; (e) R. Wang, X. Liu, A. Huang, W. Wang, Z. Xiao and L. Zhang, *Inorg. Chem.,* 2016, **55**, 1782; (f) W. Xie, W.-W. He, S.-L. Li, K.-Z. Shao, Z.-M. Su and Y.-Q. Lan, *Chem. Eur. J.,* 2016, **22**, 17298; (g) Z. Hu, B. J. Deibert and J. Li, *Chem. Soc. Rev*., 2014, **43**, 5815 and references therein; (h) N. Venkatramaiah, S. Kumar and S. Patil*, Chem. Commun*., 2012, **48**, 5007; (i) H. Xu, F. Liu, Y. Cui, B. Chen and G. Qian, *Chem. Commun*., 2011, **47**, 3153; (j) S. S. Nagarkar, B. Joarder, A. K. Chaudhari, S. Mukherjee and S. K. Ghosh, *Angew. Chem. Int. Ed*., 2013, **52**, 2881; (k) S. R. Zhang, D. Y. Du, J. S. Qin, S. J. Bao, S. Li, W. W. He, Y. Q. Lan, P. Shen and Z. M. Su, *Chem. Eur. J.,* 2014, **20** , 3589.

19 (a) X.Y. Wang, A. Del Guerzo and R. H. Schmehl, *Chem. Commun.* 2002, 2344. (b) S. Vaidya, C. Johnson, X. Y. Wang, R. H. Schmehl , *J. Photochem. Photobiol. A,* 2007, **187**, 258; (c) S. K. Chung, Y. R. Tseng, C. Y. Chen and S. S. Sun, *Inorg. Chem.,* 2011, **50**, 2711; (d) P. F. Shi, Q. Jiang, H. C. Duan and D. Q. Wang, *Chinese Chemical Letters,* 2014, **25**, 586; (e) L. S. Natrajan, A. Toulmin, A. Chew and S. W. Magennis, *Dalton Trans.,* 2010, **39**, 10837; (f) S. Righetto, S. Rondena, D. Locatelli, D. Roberto, F. Tessore, R. Ugo, S. Quici, S. Roma, D. Korystov and V. I. Srdanov, *J. Mater. Chem.,* 2006, **16**, 1439; (g) Z. J. Hu, J. X. Yang, Y. P. Tian, H. P. Zhou, X. T. Tao, G. B. Xu, W. T. Yu, X. Q. Yu and M. H. Jiang, *J. Mol. Struct.,* 2007, **839**, 50; (h) A. Sil, A. Maity, D. Giri and S. K. Patra, *Sens and Actuators B,* 2016, **226***,* 403. (i) P. Song, S. G. Sun, S. Wang, F. C. Ma, Y. Q. Xu and X. J. Peng, *Spectrochim. Acta, Part A,* 2011, **81**, 283; (j) W. Jun, X. Quan-qing, C. Shao-ming, Z. Hui-miao, F. Wen-fu, *Imaging Science and Photochemistry*, 2009, **27**, 8.

20 F. Kröhnke, *Synthesis* 1976, **1**, 1.

21 R. C. Wu, P. I. Shih, C. L. Wang and C. S. Hsu, *J. Polym. Sci., Part A: Polym. Chem.,* 2012, **50**, 696.

22 J. R. Lakowicz, *Principles of Fluorescence Spectroscopy*; 3rd edition; Springer Science: New York, 2006.

23 (a) J. A. Banal, J. M. White, K. P. Ghiggino and W. H. Wong, *Nat. Sci. Rep.,* 2014, **4**, 4635; (b) A. S. Shetty, J. Zhang and J. S. Moore, *J. Am. Chem. Soc.,* 1996, **118**, 1019. (c) L. I. Markova, V. Malinovski, L. D. Patsenker and R. Haner, *Chem. Commun.,* 2013, **49**, 5298; (d) Y. Okazawa, K. Kondo, M. Akita and M. Yoshizawa, *J. Am. Chem. Soc.,* 2015, **137**, 98; (e) Y. Hong, J. W. Y. Lama and B. Z. Tang, *Chem. Commun.,* 2009, 4332 and references there in.

24 (a) W. Wu, S. Ye, L. Huang, L. Xiao, Y. Fu, Q. Huang, G. Yu, Y. Liu, J. Qin, Q. Lia and Z. Li, *J. Mater. Chem*., 2012, **22**, 6374; (b) A. Qin, J. W. Y. Lam, L. Tang, C. K. W. Jim, H. Zhao, J. Sun and B. Z. Tang, *Macromolecules,* 2009, **42**, 1421.

25 Y. Long, H. Chen, Y. Yang, H. Wang, Y. Yang, N. Li, K. Li, J. Pei and F. Liu, *Macromolecules,* 2009, **42**, 6501.

26 J. Hou, Z. Tan, Y. Yan, Y. He, C. Yang and Y. Li, *J. Am. Chem. Soc*., 2006, **128**, 4911.

27 (a) G. H. Kim, R. Lampande, B. Y. Kang, H. W. Bae, J. Y. Lee, J. H. Kwon and J. H. Park, *Org. Electron*., 2016, **31**, 11; (b) C. G. Zhen, Z. K. Chen, Q. D. Liu, Y. F. Dai, R. Y. C. Shin, S. Y. Chang and J. Kieffer, Adv. Mater., 2009, **21**, 2425; (c) H. M. Shih, R. C. Wu, P. I. Shih, C. L. Wang and C. S. Hsu*, J. Polym. Sci., Part A: Polym. Chem*., 2012, **50**, 696.

28 (a) Z. Liu, W. He and Z. Guo, *Chem. Soc. Rev.,* 2013, **42**, 1568; (b) R. M. Manez and F. Sancenon, *Chem. Rev.,* 2003, **103**, 4419; (c) A. P. D. Silva, H. Q. N. Gunaratne, T. Gunnlaugsson, A. J. M. Huxley, C. P. McCoy, J. T. Rademacher and T. E. Rice, *Chem. Rev.,* 1997, **97**, 1515.

View Article Online
DOI: 10.1039/C7TC04178K

Arylene-vinylene Terpyridine Conjugates: Highly Sensitive, Reusable and Simple Fluorescent Probes for the Detection of Nitroaromatics

Amit Sil,[a] Dipanjan Giri,[a] and Sanjib K. Patra*[a]

TOC

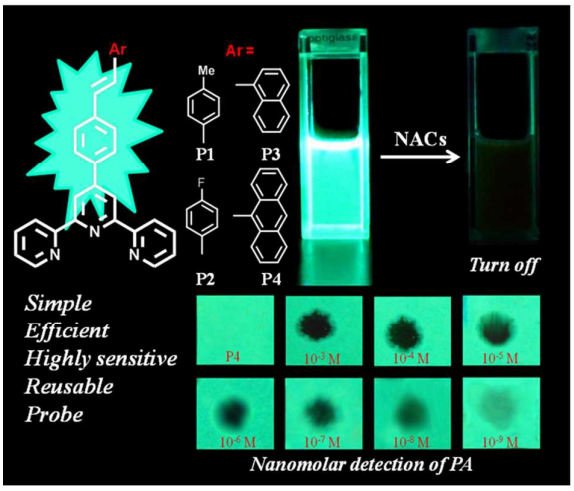

A series of highly emissive arylene-vinylene terpyridine conjugates have been developed for the detection of nitroaromatic (NAC) explosives as efficient and reusable fluorescent probes.